



SEMI-EMPIRICAL MODEL FOR PREDICTING THE SPECIFIC ENERGY CONSUMPTION IN REVERSE OSMOSIS DESALINATION

Reda Askouri¹, Mohamed Moussetad¹, Hind Ennasri¹, Rhma Adhiri¹

¹Laboratory of Engineering and Materials, Faculty of Science Ben M'sick, Hassan II University of Casablanca,

B.P.7955 Casablanca, Morocco, askouri.reda.univh2c@gmail.com

Abstract: The first goal of this study is to examine the performance of a semi-empirical model used for calculating specific energy consumption (SEC) in reverse osmosis desalination. We have introduced a simulation tool (SEC_{SM}) to compare this semi-empirical model (SEC_{SEM}) and the SEC_{SM} . It's worth noting that the simulation model is open source and can be easily integrated easily with other software tools. For this comparison, we explored a temperature range T ($10^{\circ}C - 22^{\circ}C - 35^{\circ}C$), recovery rate R from 30% to 65%, and a pump efficiency range of $\gamma_{HPP} \sim 78\%$ to 98%. An increase in these parameters leads to a decrease in SEC (both SEC_{SEM} and SEC_{SM}) for systems without energy recovery devices (ERD). However, the introduction of an ERD results in a variable change in SEC_{SEM} . Under specific conditions of $35^{\circ}C$, a pump efficiency of 98%, and an R of 65%, the SEC_{SEM} reaches its minimum values. In the case of the two-stage unit (TS), the SEC_{SEM} and SEC_{SM} models converge to the same value of 0.28 KWh/m^3 . Meanwhile, for the single-stage unit (SS), the values are 0.4 KWh/m^3 and 0.39 KWh/m^3 , respectively. Regarding the unit equipped with the BW 400 34 and SW HF 085 31 membranes, in both SS and TS configurations, the energy consumption for both models converge towards the values 0.71 KWh/m^3 , 0.70 KWh/m^3 , and 0.95 KWh/m^3 , 0.94 KWh/m^3 respectively. In the second part of this paper, a comparative study to validate this semi-empirical model without ERD against experimental data was conducted. The SEC_{SEM} showed values very close to the experimental results. The findings are discussed below.

Key words: Brackish water, Specific energy consumption, Reverse osmosis, Experimental study, The Semi-Empirical model

1. INTRODUCTION

Water is the most crucial resource for the survival of all life forms on the planet [1],[2]. Earth is blessed with an abundant water supply, with approximately 94% of its existing as seawater in the oceans, while the remaining 6% is classified as freshwater. Freshwater, which is vital for consumption and various purposes, accounts for approximately 72% of the planet's water supply and is primarily found underground, with the remaining 27% stored in glaciers [3]. Water is categorized based on its salinity levels, with seawater having a high concentration of total dissolved solids (TDS) at around 35000 mg/L or more. Brackish water, or water with moderate salinity, falls within the range of $1,000$ to $15,000 \text{ mg/L}$ of TDS concentration. Freshwater, characterized by low salinity, contains less than 500 mg/L of TDS. A comprehensive analysis of the different types of water has been documented in detail by [4]. Due to the rapid expansion of the global population and the increasing demand for water [5], the need for sustainable water sources is expected to rise sharply over the next decade. This has prompted research aimed at improving various desalination processes, including reverse osmosis (RO) [6], liquid-liquid extraction, multi-stage flash distillation,

and membrane distillation [7]. More than half of the world's freshwater is produced using the most widely adopted desalination method, namely RO [8]. The range of applications for RO membrane technology has expanded considerably in recent years, including large-scale desalination of seawater and brackish water for drinking water production, industrial process water conditioning, and treatment of various effluents for clean water reuse. The current focus is on applying sustainability criteria, including minimising the specific energy consumption of product water [9].

However, RO is known to be energy-intensive due to the high hydraulic pressure required as the driving force [10],[11]. To address this issue, various measures have been implemented to reduce the specific energy consumption of the RO process. These include the development of RO membranes with exceptionally high permeability [12], the use of pressure recovery devices such as efficient ERDs [13], improvements in the geometric design of spiral-wound membrane modules for RO, and the mitigation of fouling effects through chemical pretreatment [14],[15]. The sustainability of the overall process in terms of SEC [16], is commonly expressed as Kilowatt-hours (KWh) per cubic meter of

water produced, which is a key parameter for evaluating the performance of water treatment processes [17].

Recent literature contains numerous research papers focusing on specific energy consumption in reverse osmosis facilities. These papers can be categorized into two types: those that use data from operational facilities [18],[19], and those that rely on theoretical analysis [20],[21]. While the first type of data is valuable, it often presents averaged energy consumption values over an unspecified range of process parameters, lacking detailed information on process design and operating conditions. Existing theoretical studies provide relevant insights into energy consumption, either in a general sense or within optimisation frameworks (e.g.[20],[22],[23]). However, a thorough examination of the specific contributions to energy usage is still lacking [21].

The primary objective of this paper is to predict the behaviour of the SEC_{SEM} across various scenarios involving a reverse osmosis unit for brackish water. The calculations from the SEC_{SEM} are performed using the Python language. Additionally, the energy recovery system for reverse osmosis is included in the simulation solely to compare the values obtained with the SEC_{SEM} formula in the presence of an ERD. During the simulation, we employed two distinct membrane types, namely BW 400 30 and SW HR 085 31, within the context of brackish water. This selection was made to highlight disparities in energy fluctuations and to observe the evolution curves of the SEC_{SEM} . The analysis is typically carried out using a comprehensive software model (Lanxess Lewaplast design), which allows for the simulation of different water characteristics to calculate the SEC_{SM} in RO plants operating under stable conditions [24]. Finally, we will rely on experimental data from brackish water treated through reverse osmosis to validate this semi-empirical model. A comparative study will also be conducted between the experimental data and the SEC_{SEM} .

2. INPUT DATA FOR THIS STUDY

2.1 Composition of brackish feed water and parameters of operation

Table 1 displays the mineral composition of water extracted from the SAFI region of Morocco. The goal is to meticulously outline the precise mineral composition of the brackish water in question, providing a solid foundation for comparing the simulation results with the data generated by the semi-empirical model. In this research endeavour, as mentioned earlier, different pressure levels were applied to enhance the adaptability of the semi-empirical formula to diverse pressure conditions. According to the Lewaplast simulator model, the system is divided into two membrane types arranged in a spiral-wound configuration within a standard 7-element pressure vessel. The input data used for the case study, summarised in Table 2, represent typical

conditions and module design parameters commonly encountered in such applications.

Table 1. Feed brackish water

Element	Values
pH	8.37
Ca ²⁺ (mg/L)	57.52
Mg ²⁺ (mg/L)	52.65
Na ⁺ (mg/L)	209.73
K ⁺ (mg/L)	4.7
Cl ⁻ (mg/L)	340-380
HCO ₃ ⁻ (mg/L)	111.9
So ₄ ²⁻ (mg/L)	160
SiO ₂ (mg/L)	4.57
Co ₃ ²⁻ (mg/L)	2.15
Conductivity (us/cm)	1656.76

Table 2. Data used for this study

Characteristics of the feed brackish water	Value	
Salinity	1000.48 mg/L	
Parameters of operation		
Feed Flow Q_F	200.00 m ³ /h	
Recovery rate R	30% – 65%	
Temperature T	10°C – 35°C	
Membrane design	BW 400 34	SW HF 085 31
Type of membrane	Lewabrane	Lewabrane
Membrane polymer	Composite Polyamide	Composite Polyamide
Membrane active area	37 m ²	7.4 m ²

3. SPECIFIC ENERGY CONSUMPTION FROM THE SEMI-EMPIRICAL FORMULA MODEL

3.1 Specific energy consumption in the RO process

Energy consumption in reverse osmosis refers to the amount of energy required to produce a certain volume of treated water using the RO process. It is commonly expressed in kilowatt-hours per cubic meter (KWh/m³) or kilowatt-hours per gallon (KWh/gal). It is important to note that SEC can vary significantly depending on the specific application and the RO system being used [25]. Advanced technologies, system optimisation, and improvements in membrane technology have led to more energy-efficient RO systems in recent years, reducing

SEC and making RO a cost-effective and sustainable water treatment option.

3.2 Theoretical formula model of specific energy consumption without an ERD system

Figure 1 shows the SS and TS reverse osmosis units in the absence of an ERD. The formula of the semi-empirical model used to calculate the specific energy consumption for reverse osmosis systems without an ERD is based on similar models found in the literature [19],[24]. Furthermore, we have refined this model to ensure that the presented results align with both simulation and experimental data in an acceptable manner. Generally, the semi-empirical formula can be expressed as follows:

$$SEC_{SEM} = \frac{P_s \times \delta_{rrm}}{R \times \gamma_{HPP}} \quad (1)$$

P_s is the supply pressure in Pascal, R is the recovery rate and γ_{HPP} is the high-pressure pump efficiency.

$$\delta_{rrm} = \frac{3.6 \times 10^{-5} \times \pi_{os}}{C_{AD}} \quad (2)$$

$$C_{AD} = \Delta P \times N_{ME,RO} \times N_{S,RO} \quad (3)$$

π_{os} represents the osmotic pressure, while C_{AD} serves as an adjustment factor to refine the specific energy consumption calculations within the semi-empirical model. The selection of this parameter is based on multiple tests and literature focused on specific energy consumption. It is a comprehensive term that includes various components intended to have an indirect influence on energy consumption. Among these factors, we must consider the pressure drops within the membrane elements in the pressure tubes [27], the membrane elements that can be installed in the pressure tubes, and the stages that can be implemented in a reverse osmosis system [28]. In this case, based on the calculations related to the adjustment term, its value is set at 0.03, which represents a numerical value derived from the factors mentioned above. Finally, the theoretical formula for specific energy consumption is written as follows:

$$SEC_{SEM} = \frac{P_s \times 0.03}{R \times \gamma_{HPP}} \quad (4)$$

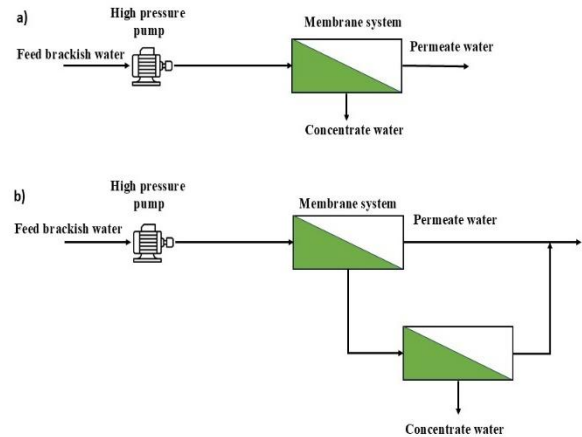


Figure 1 Brackish feed water RO treatment plant.

(a) Itemized single-stage unit without ERD;

(b) Unit with two stages without ERD

During the RO process, the feed water is pressurised and forced through the semi-permeable RO membrane. The membrane acts as a barrier, allowing water molecules to pass through while blocking dissolved solids, contaminants, and minerals [29]. As a result, two streams of water are produced: purified water (permeate) and retentate (reject or brine). The feed water enters the RO system as a single stream and exits as either concentrated or permeate water in a one-stage RO system. The concentrate from the first stage serves as the feed water for the second stage in a two-stage RO system. The filtered water collected in the first stage is combined with the treated water obtained in the second stage. Additional stages enhance system efficiency. In RO, concentrate water refers to the water that carries the majority of the impurities and contaminants rejected by the RO membranes [30]. This concentrated water exits the RO unit at high pressure due to the operating conditions of the system.

3.3 Single-stage / Two stages RO with ERD system

In Figure 2, a reverse osmosis unit with an ERD is configured to incorporate a mechanism for recovering and reusing energy that would otherwise be wasted during the RO process. The ERD helps improve the overall energy efficiency of the RO system by reducing the amount of energy required to operate it [31]. An energy recovery device, such as a pressure exchanger or turbine, is integrated into the RO system to capture energy from the brine stream [32]. The ERD works by transferring energy from the pressurised concentrate water to the incoming feed water, thereby reducing the overall energy consumption of the system. A pressure exchanger is a device that utilises the pressure energy from the brine stream to pressurise the incoming feed brackish water. It operates through a process of hydraulic energy exchange, where the high-pressure feed

brackish water passes through separate chambers with a semipermeable membrane. This process allows energy to be transferred from the brine to the feed brackish water without direct mixing. For the semi-empirical formula of energy consumption in the presence of an ERD, the difference between eq. 3 and this equation lies in the introduction of the ERD efficiency term. As for the adjustment term, the same calculations are applied to this equation. In general, the equation in the presence of energy recovery is written as follows:

$$SEC_{SEM} = \frac{P_s \times (1 - \gamma_{ERD} \times (1 - R)) \times \delta_{rrm}}{\gamma_{HPP} \times R} \quad (5)$$

γ_{ERD} provides the ERD efficiency. The final formula for theoretical energy consumption is as follows:

$$SEC_{SEM} = \frac{P_s \times (1 - \gamma_{ERD} \times (1 - R)) \times 0.03}{\gamma_{HPP} \times R} \quad (6)$$

In this study, regarding the comparison between the semi-empirical model and the simulation, we chose an efficiency of 98% for the pump and the energy recovery device. For the efficiencies of 78% and 88%, we have listed the best values obtained for energy consumption in the tables.

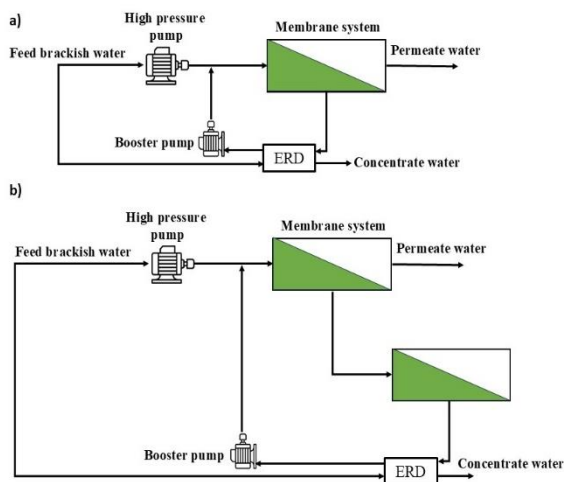


Figure 2 Brackish feed water RO treatment plant.

- (a) itemized single-stage unit with ERD;
- (b) Unit with two stages in the presence of ERD

4. RESULTS

This section includes a comparative analysis between the semi-empirical model and the simulation. Additionally, a comparison of experimental models is presented in this segment. To predict the behaviour of this semi-empirical model, we conduct a parametric analysis encompassing several influential factors affecting specific energy consumption. This article references multiple parametric studies investigating

variations in specific energy consumption [25],[33],[34]. In our case, simulation serves as a means to corroborate the calculations presented, ensuring a reliable basis for comparison with the values derived from this semi-empirical model for reverse osmosis systems, both with and without energy recovery. Figure 3 illustrates the changes in SEC_{SEM} across various temperature levels. In the case of an SS unit, the SEC_{SEM} results in higher energy consumption compared to a TS unit [35]. The introduction of two membranes leads to a disparity in energy consumption. The SEC_{SEM} applied in the BW 400 34 membrane demonstrates lower energy consumption compared to the SW HF 085 31 membrane. Furthermore, a strong alignment between the SEC_{SEM} and the SEC_{SM} is evident, with this alignment becoming particularly pronounced in the context of TS energy variation. The same principle applies to energy variation in an SS unit: the SEC_{SEM} exhibits a correlation with the SEC_{SM} . This correlation is prominently demonstrated in Figure 3.e, where the model for a system without energy recovery closely mirrors the values presented by the simulation. On the contrary, the SEC_{SEM} shows a decrease in energy consumption for both membrane types as the conversion ratio increases, reaching its tipping point at $R = 65\%$.

Notably, temperature substantially impacts energy variation in the SEC_{SEM} , a dynamic observed in both SS and TS units. Furthermore, what is truly remarkable is the consistent superiority of the SEC_{SEM} over the SEC_{SM} across every curve depicted in this figure. This phenomenon holds for all scenarios, encompassing both membrane types and stages within the study. It underscores the robustness and effectiveness of the SEC_{SEM} employed in this comprehensive analysis. Table 3 provides a detailed comparison of the optimum energy consumption values between the SEC_{SEM} and SEC_{SM} at $R = 65\%$. This comparison encompasses various temperature settings and pump efficiencies. What is particularly striking is that, regardless of these variables, the difference between the two models remains fixed at 0.03 KWh/m^3 . This consistency underscores the superiority of the SEC_{SEM} for specific energy consumption in reverse osmosis without energy recovery, as it consistently outperforms the SEC_{SM} in generating more favourable comparative results.

The inclusion of an energy recovery system impacts the SEC_{SEM} and its evolution within both SS and TS reverse osmosis units. In this instance, as shown in Figure 4, the simulation model surpasses the semi-empirical model across both membrane types and stages. Additionally, a noteworthy observation is that, with increasing temperature, the disparity between the SEC_{SEM} and the SEC_{SM} becomes more pronounced, particularly at $R = 30\%$. Another point to highlight is that, within both SS and TS feeds, the SEC_{SEM} exhibits almost a linear progression for both membrane types. This suggests that the inclusion of the energy recovery term significantly impacts the results obtained from eq.5. Nevertheless, as the conversion rate increases, a noteworthy alignment between the SEC_{SEM} and the

SEC_{SM} emerges, particularly evident at $10^{\circ}C$. Regarding the evolution of the SEC_{SEM} , it is noteworthy that there is no opposing trend between the SEC_{SEM} and the SEC_{SM} when both the conversion rate and temperature variation increase. This is because energy consumption consistently follows an upward trajectory in both computational models, without any indication of a decrease. Nonetheless, the implementation of ERD notably influences the SEC_{SEM} . Specifically, it leads to a divergence in values at $R=30\%$ and an affinity between the SEC_{SEM} and the SEC_{SM} at $R=65\%$ provided in Table 4. This divergence and affinity signify the dynamic interplay between the semi-empirical model and practical results when considering the influence of energy recovery on specific energy consumption in reverse osmosis processes.

To assess the practical significance of specific electrical energy consumption, an extensive experimental study was conducted to measure this parameter, as mentioned in reference [36]. To validate this model, a comparison between the values obtained from the experimental model and the SEC_{SEM} is outlined in equation 3. The results of this investigation are presented in Table 5.

The data in Table 5 indicates a notable correlation between the increase in feed concentration and a corresponding rise in specific experimental energy consumption. This trend is consistent with the observations made for the semi-empirical model without ERD. Specifically, when the feed concentration is at 2 g/L, the experimental energy consumption reaches its minimum at 0.568 kWh/m³, and the SEC_{SEM} closely mirrors this value at 0.568 kWh/m³. At higher concentrations, such as 3 g/L and 4 g/L, both the experimental measurements and the SEC_{SEM} show a similar pattern, reaching 0.64 kWh/m³ and 0.634 kWh/m³, as well as 0.74 kWh/m³ and 0.748 kWh/m³, respectively.

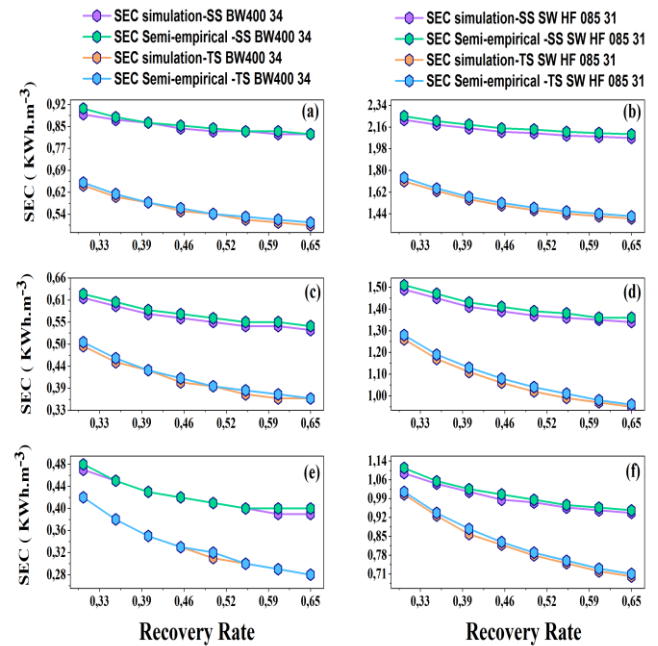


Figure 3 SEC_{SEM} and SEC_{SM} variations based on recovery rate in single and two-stage systems without ERD across different temperatures and $\gamma_{HPP} = 98\%$. (Curves a and b depend on $10^{\circ}C$ / Curves c and d depend on $22^{\circ}C$ / Curves e and f depend on $35^{\circ}C$).

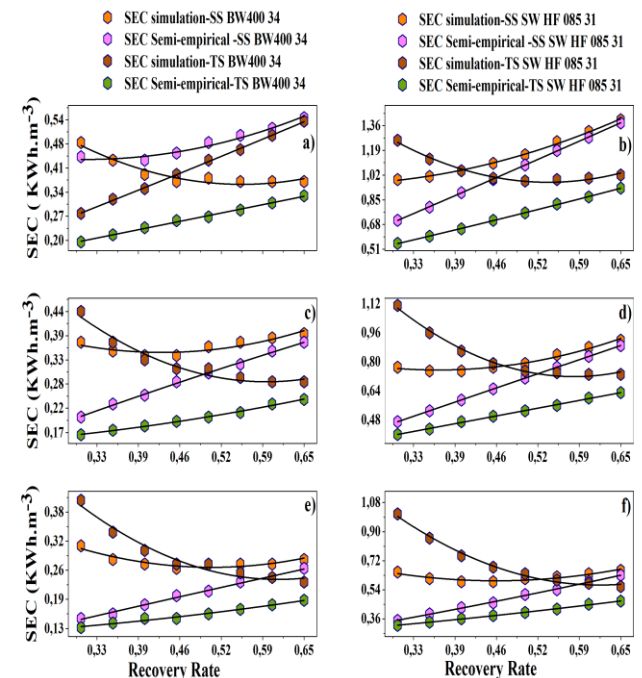


Figure 4 Curves fitting of SEC_{SEM} and SEC_{SM} variations based on recovery rate in single and two-stage systems with ERD across different temperatures and $\gamma_{ERD} = \gamma_{HPP} = 98\%$. (Curves a and b depend on $10^{\circ}C$ / Curves c and d depend on $22^{\circ}C$ / Curves e and f depend on $35^{\circ}C$).

Table 3. Comparison values between SEC_{SEM} and SEC_{SM} for a system without ERD at R= 65%.

BW 400 34					
T (°C)	Y _{HPP}	SEC_{SM-SS}	SEC_{SEM-SS}	SEC_{SM-TS}	SEC_{SEM-TS}
10	0.78	1.01	1.03	0.63	0.63
	0.88	0.9	0.91	0.55	0.56
	0.98	0.8	0.82	0.5	0.51
22	0.78	0.67	0.68	0.45	0.45
	0.88	0.6	0.6	0.4	0.4
	0.98	0.53	0.54	0.36	0.36
35	0.78	0.49	0.5	0.35	0.36
	0.88	0.43	0.44	0.31	0.32
	0.98	0.39	0.4	0.28	0.28
SW HF 085 31					
T (°C)	Y _{HPP}	SEC_{SM-SS}	SEC_{SEM-SS}	SEC_{SM-TS}	SEC_{SEM-TS}
10	0.78	2.6	2.64	1.75	1.78
	0.88	2.31	2.34	1.55	1.58
	0.98	2.07	2.01	1.4	1.42
22	0.78	1.68	1.7	1.19	1.21
	0.88	1.49	1.51	1.05	1.07
	0.98	1.34	1.36	0.95	0.96
35	0.78	1.18	1.2	0.88	0.9
	0.88	1.05	1.06	0.78	0.79
	0.98	0.94	0.95	0.7	0.71

Table 4. Comparison values between SEC_{SEM} and SEC_{SM} for a system with ERD at R= 65%.

BW 400 34					
T (°C)	Y _{HPP}	SEC_{SM-SS}	SEC_{SEM-SS}	SEC_{SM-TS}	SEC_{SEM-TS}
10	0.78	0.69	0.75	0.47	0.46
	0.88	0.61	0.63	0.41	0.39
	0.98	0.55	0.54	0.37	0.33
22	0.78	0.47	0.50	0.35	0.33
	0.88	0.42	0.42	0.31	0.28
	0.98	0.39	0.37	0.28	0.24
35	0.78	0.35	0.36	0.29	0.26
	0.88	0.31	0.31	0.25	0.22
	0.98	0.28	0.26	0.23	0.19
SW HF 085 31					
T (°C)	Y _{HPP}	SEC_{SM-SS}	SEC_{SEM-SS}	SEC_{SM-TS}	SEC_{SEM-TS}
10	0.78	1.76	1.92	1.28	1.29
	0.88	1.65	1.62	1.14	1.09
	0.98	1.4	1.38	1.02	0.93
22	0.78	1.16	1.24	0.91	0.9
	0.88	1.03	1.04	0.81	0.74
	0.98	0.92	0.89	0.73	0.63
35	0.78	0.83	0.87	0.71	0.65
	0.88	0.74	0.74	0.63	0.55
	0.98	0.66	0.63	0.56	0.47

Table 5. The comparative study between experimental measures (SEC_{EXP}) and SEC_{SEM}

Reference	Feed salinity (g/l)	SEC_{EXP} (kWh/m ³)	SEC_{SEM} (kWh/m ³)	Errors (%)
[36]	2	0.56	0.568	1.41
	3	0.64	0.634	0.95
	4	0.74	0.748	1.07

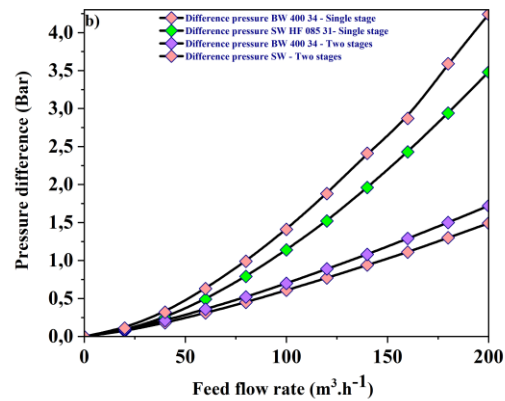
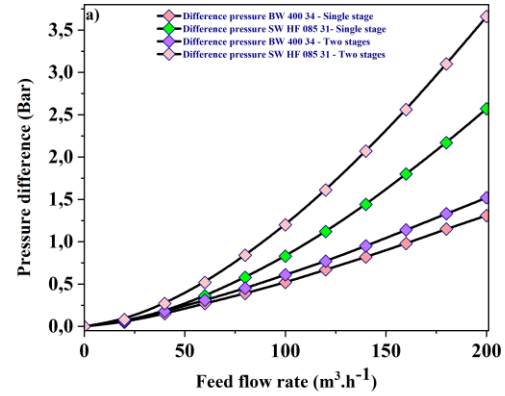


Figure 5 Difference pressure across pressure tube in reverse osmosis unit.

- a) itemized system without ERD;
- b) itemized system with ERD.

5. Discussion

In this section, it becomes evident that temperature and conversion rate influence the energy fluctuations within the SEC_{SEM} . Notably, it is imperative to observe that as temperature varied, the SEC_{SEM} consistently exhibited a stable progression, ultimately yielding optimal outcomes for both membrane types at a temperature of 35°C.

In the context of the membranes examined in this research, it is noteworthy that the SW HF 085 31 exhibits higher energy consumption compared to the BW 400 34. This disparity in energy consumption can be attributed to differences in permeability characteristics between the two membrane types, as explained in the scientific literature review referenced previously [37].

In Figures 3e and 3f, temperature exerts a notable indirect influence on the SEC_{SEM} in both membranes (in SS and TS units).

The rise in temperature leads to a decrease in pressure as a consequence of the reduction in water

viscosity, which, in turn, enhances water injection into the membranes [38].

Furthermore, for the BW 400 34 membranes, when the conversion rate reaches 65%, the SEC_{SEM} attains optimal values of 0.4 kWh/m³ and 0.28 kWh/m³ for the SS and TS stages, respectively. The same scenario applies to the SW HF 085 31 membrane, which achieves optimal values of 0.95 kWh/m³ and 0.71 kWh/m³, respectively. There is a corresponding decrease in SEC_{SEM} , reflecting the inverse correlation between the conversion rate and SEC_{SEM} . Conversely, within the SS configuration, SEC_{SEM} exceeds that of the TS configuration, primarily due to the higher Ps: R ratio associated with the SS compared to the TS units. Moreover, the SEC_{SEM} from SS aligns with existing literature, as demonstrated by Alhathal Alanezi et al., who also examined energy consumption variations in conversion rates, typically within the range of 36% to 60% [31]. Notably, when considering conversion rates below 50%, the energy consumption behaviour observed in our study is consistent with their findings, with variations primarily arising from differences in water types and treatment preferences. Furthermore, it is worth noting that previous research has indicated that within the conversion rate range of 20% to 50%, the energy consumption in TS units surpasses that of SS units [39]. However, beyond this interval, the behaviour observed aligns with our findings as presented by the semi-empirical model. This disparity can likely be attributed to the presence of the pressure drop factor considered within the scope of this investigation. Regarding the difference in pressure across pressure tubes, Figure 5 has been included specifically to elucidate our findings with a high degree of reliability. In Figure 5a, during the increase in feed flow, it is clear that the SW HF 085 31 membrane in both stages experience a pressure difference across the pressure tube of 3.66 Bars and 2.57 Bars more than the BW 400 34 membrane, which explains the higher energy consumption and corroborates the outcomes depicted in Figure 3.

In Figures 4e and 4f, the SEC_{SEM} in the presence of an ERD shows that the increase in SEC_{SEM} can be attributed to the interplay of two factors: energy recovery efficiency and the conversion rate. Furthermore, the SEC_{SEM} in an SS exceeds that in a TS setup due to the applied supply pressure, which serves to augment energy demand.

Regarding the BW 400 34 and SW HF 085 31 membranes, as the conversion rate increases, the SEC_{SEM} in an SS experiences an elevation of 42.31% and 44.44%, respectively.

For the TS unit, the percentage increase in energy consumption is 31.58% and 31.91%, respectively. Moreover, with the assistance of figure 5b, it is observed that the difference in pressure across the pressure tube influences this semi-empirical energy variation between the two stages of reverse osmosis. We have encountered a similar study concerning the impact of an ERD on the feed flow.

The results presented in this study, considering an efficiency of 95% for the ERD, align with the outcomes mentioned for the SEC_{SEM} with an efficiency of 98% [31].

Another similar study published last year discussed a system that addresses the variation of specific energy consumption in the context of seawater energy recovery using a direct osmosis system. The energy variations align with our semi-empirical model, with the variations attributed to differences in the type of water being treated and the specific hybrid system employed in the study [33].

The data from Table 5 underscore a notable trend: as the concentration of the feed increases, both the SEC_{EXP} and the SEC_{SEM} model demonstrate.

This correlation is linked to the escalating pressure requirements associated with higher salinity levels, highlighting the necessity for increased energy to facilitate the desalination process [40], [41], [42]. Another significant observation is the remarkable proximity between the experimental and semi-empirical values.

This proximity highlights the robustness and accuracy of the models used in this study, suggesting that the semi-empirical model effectively predicts system behavior in response to variations in feed salinity. Furthermore, it is worth mentioning that the error percentage remains consistently below 1.5% for salinities of 2, 3, and 4 g/L, as indicated in Table 5.

This finding accentuates the precision and reliability of the values generated by this model, reaffirming its suitability for the specific water treatment scenario under investigation.

This finding indicates that the semi-empirical model, in the absence of energy recovery, predicts values that are very close to the experimental results due to its alignment with the type of water being treated in this study.

6. CONCLUSION

In the context of this article, we have introduced a new semi-empirical model designed to compute the specific energy consumption for both single reverse osmosis units, in scenarios with and without an energy recovery device. The aim is to establish the boundaries of this model within the mentioned cases. The simulation conducted in this study served as a comparative tool, followed by the validation of this model. The simulation was carried out using a well-established and dependable tool, ensuring that the values obtained are robust and credible. This step was essential for incorporating the simulation results into the subsequent discussion of the theoretical model. With the assistance of the parameters mentioned above, we have obtained the following results:



- In a system without an ERD, the SEC_{SEM} for the BW 400 30 membrane is lower than that for the SW HF 085 31 membrane.
- At $T = 10^{\circ}C$, the SEC_{SEM} for the BW 400 34 membranes exhibits a strong alignment with the simulation, reaching 0.51 kWh/m^3 at conversion rates of $R = 55\%$ and 60% for the TS unit.
- When the temperature reaches $35^{\circ}C$, the variation in SEC_{SEM} closely aligns with the simulation in both stages as the conversion rate increases.
- Regarding the SW HF 085 31 membranes, the behaviour of the semi-empirical energy consumption converges with the simulation in both stages at various temperatures.
- The SEC_{SEM} indicates that energy consumption in an SS unit is higher than in a TS unit for both membranes at different temperatures.
- For both membranes in SS feeding, the evolution of the SEC_{SEM} exhibits a similar increasing trend and aligns with the SEC_{SM} when the conversion rate reaches 60% .
- For the TS unit, a difference between the SEC_{SEM} and the SEC_{SM} is observed at the minimum conversion rates.
- After comparing with previous studies, our semi-empirical model aligns with the existing literature that focuses on the same system presented in this study.
- For brackish water reverse osmosis prototypes, the semi-empirical model yields values that are very close to the experimental measurements.
- In comparison with the experimental study, the semi-empirical model shows values that are very close, with a very low margin of error for concentrations of 2, 3, and 4 g/L .

Regarding the semi-empirical model and the presence of an ERD, we couldn't find a prototype with a recovery system to compare with the experimental measurements.

However, in this case, the model has the same parameters as in the absence of energy recovery, with the difference lying in the existence of an energy recovery efficiency term.

At present, we aim to extend the application of this semi-empirical model to various scenarios and conduct multiple trials with seawater to ensure the credibility of the presented values.

The validation process involves subjecting the model to real-world conditions and a broader range of application

This multifaceted approach seeks to establish the model's validity across different water sources, including seawater, which can vary significantly in their properties and composition.

By conducting these extensive experiments and validations, we aim to demonstrate the versatility and applicability of the theoretical model in a variety of

practical settings, ultimately bolstering its utility and scientific rigor.

7. REFERENCES

- [1] T. Ning et al., 2023 « *Precipitation changes and its interaction with terrestrial water storage determine water yield variability in the world's water towers* », *Sci. Total Environ.*, vol. 880, p. 163285, July.
- [2] D. Hassane, A. Didi, D. Ilham, M. J. Derkaoui, et Y. Mohammed, 2024, « *The First Investigation on the Radiotoxicity Risks Associated with Ingesting Radium in Drinking Water from the Oujda Region-Morocco and some Bottled Mineral Waters.* », *Appl. Radiat. Isot.*, p. 111356, May.
- [3] M. A. Alghoul, P. Poovanaesvaran, K. Sopian, et M. Y. Suleiman, 2009, « *Review of brackish water reverse osmosis (BWRO) system designs* », *Renew. Sustain. Energy Rev.*, vol. 13, n° 9, p. 2661-2667, Dec.
- [4] S. El-Manharawy et A. Hafez, 2001, « *Water type and guidelines for RO system design* », *Desalination J.*, vol. 139, n° 1, p. 97-113, September.
- [5] Y. Dai et Z. Liu, 2023, « *Spatiotemporal heterogeneity of urban and rural water scarcity and its influencing factors across the world* », *Ecol. Indic.*, vol. 153, p. 110386, September.
- [6] T. Pluym, C. García-Timmermans, S. Vervloet, R. Cornelissen, N. Boon, et B. D. Gussemé, 2023, « *Flow cytometry for on-line microbial regrowth monitoring in a membrane filtration plant: pilot-scale case study for wastewater reuse* », *Environ. Sci. Water Res. Technol.*, vol. 9, n° 8, p. 2128-2139.
- [7] P. G. Youssef, R. K. AL-Dadah, et S. M. Mahmoud, 2014, « *Comparative Analysis of Desalination Technologies* », *Energy Procedia*, vol. 61, p. 2604-2607, January.
- [8] A. Altaee, G. Zaragoza, et H. R. van Tonningen, 2014, « *Comparison between Forward Osmosis-Reverse Osmosis and Reverse Osmosis processes for seawater desalination* », *Desalination*, vol. 336, p. 50-57, March.
- [9] A. J. Karabelas, C. P. Koutsou, D. C. Sioutopoulos, K. V. Plakas, et M. Kostoglou, « *Desalination by Reverse Osmosis* », in *Sustainable Membrane Technology for Water and Wastewater Treatment*, A. Figoli et A. Criscuoli, Éd., in *Green Chemistry and Sustainable Technology.*, Singapore: Springer, 2017, p. 155-199.



- [10] Z. Mo, D. Li, et Q. She, 2022, « *Semi-closed reverse osmosis (SCRO): A concise, flexible, and energy-efficient desalination process* », *Desalination*, vol. 544, p. 116147, December.
- [11] A. K. Rao *et al.*, « A framework for blue energy enabled energy storage in reverse osmosis processes », *Desalination*, vol. 511, p. 115088, sept. 2021.
- [12] F. Dai *et al.*, « Ultrahigh water permeance of a reduced graphene oxide nanofiltration membrane for multivalent metal ion rejection », *Chem. Commun.*, vol. 56, n° 95, p. 15068-15071, December, 2020.
- [13] A. A. Alsarayreh, M. A. Al-Obaidi, A. M. Al-Hroub, R. Patel, et I. M. Mujtaba, 2020, « *Evaluation and minimisation of energy consumption in a medium-scale reverse osmosis brackish water desalination plant* », *J. Clean. Prod.*, vol. 248, p. 119220, March.
- [14] A. H. Haidari, S. G. J. Heijman, et W. G. J. van der Meer, 2018, « *Optimal design of spacers in reverse osmosis* », *Sep. Purif. Technol.*, vol. 192, p. 441-456, February.
- [15] C. J. Gabelich, M. D. Williams, A. Rahardianto, J. C. Franklin, et Y. Cohen, 2007, « *High-recovery reverse osmosis desalination using intermediate chemical demineralization* », *J. Membr. Sci.*, vol. 301, n° 1, p. 131-141, September.
- [16] N. Lior, 2017, « *Sustainability as the quantitative norm for water desalination impacts* », *Desalination*, vol. 401, p. 99-111, January.
- [17] J. Mi *et al.*, 2023, « *Experimental investigation of a reverse osmosis desalination system directly powered by wave energy* », *Appl. Energy*, vol. 343, p. 121194, August.
- [18] R. Semiat, 2008, « *Energy Issues in Desalination Processes* », *Environ. Sci. Technol.*, vol. 42, n° 22, p. 8193-8201, November.
- [19] N. Ghaffour, T. M. Missimer, et G. L. Amy, 2013, « *Technical review and evaluation of the economics of water desalination: Current and future challenges for better water supply sustainability* », *Desalination*, vol. 309, p. 197-207, January.
- [20] A. Zhu, P. D. Christofides, et Y. Cohen, 2009, « *Effect of Thermodynamic Restriction on Energy Cost Optimization of RO Membrane Water Desalination* », *Ind. Eng. Chem. Res.*, vol. 48, n° 13, p. 6010-6021, July.
- [21] B. Qi, Y. Wang, S. Xu, Z. Wang, et S. Wang, 2012, « *Operating Energy Consumption Analysis of RO Desalting System: Effect of Membrane Process and Energy Recovery Device (ERD) Performance Variables* », *Ind. Eng. Chem. Res.*, vol. 51, n° 43, p. 14135-14144, October.
- [22] A. Jiang, J. Wang, L. T. Biegler, W. Cheng, C. Xing, et Z. Jiang, 2015, « *Operational cost optimization of a full-scale SWRO system under multi-parameter variable conditions* », *Desalination*, vol. 355, p. 124-140, January.
- [23] A. Ghobeity et A. Mitsos, 2010, « *Optimal time-dependent operation of seawater reverse osmosis* », *Desalination*, vol. 263, n° 1, p. 76-88, November.
- [24] LewaPlus Calculation and Design Software, anxess.com/en/products-and-brands/brands/lewatit/lewaplus-software.
- [25] A. J. Karabelas, C. P. Koutsou, M. Kostoglou, et D. C. Sioutopoulos, 2018, « *Analysis of specific energy consumption in reverse osmosis desalination processes* », *Desalination*, vol. 431, p. 15-21, April.
- [26] A. Ruiz-García et E. Ruiz-Saavedra, 2015, « *80,000h operational experience and performance analysis of a brackish water reverse osmosis desalination plant. Assessment of membrane replacement cost* », *Desalination*, vol. 375, p. 81-88, November.
- [27] A. Ruiz-García et I. Nuez, 2021, « *A time-dependent model of pressure drop in reverse osmosis spiral wound membrane modules* », *IFAC-Pap.*, vol. 54, n° 3, p. 158-163, January.
- [28] RO-NF-FilmTec-Manual-45-D01504-en.pdf.
- [29] K. M. Sassi et I. M. Mujtaba, 2011, « *Optimal design and operation of reverse osmosis desalination process with membrane fouling* », *Chem. Eng. J.*, vol. 171, n° 2, p. 582-593, July.
- [30] K. M. Sassi et Iqbal. M. Mujtaba, « *Optimization of Design and Operation of Reverse Osmosis Based Desalination Process Using MINLP Approach Incorporating Fouling Effect* », in *Computer Aided Chemical Engineering*, vol. 29, E. N. Pistikopoulos, M. C. Georgiadis, et A. C. Kokossis, Éd., in 21 European Symposium on Computer Aided Process Engineering, vol. 29, Elsevier, 2011, p. 206-210.
- [31] A. Alhathal Alanezi, A. Altaee, et A. O. Sharif, 2020, « *The effect of energy recovery device and feed flow rate on the energy efficiency of reverse osmosis*



process », Chem. Eng. Res. Des., vol. 158, p. 12-23, June.

[32] D. Song et al., 2021, « *Demonstration of a piston type integrated high pressure pump-energy recovery device for reverse osmosis desalination system* », Desalination, vol. 507, p. 115033, July.

[33] Y. K. Goi, Y. Y. Liang, W. J. Lau, et G. A. Fimbres Weihs, 2023, « *Analysis of the effect of advanced FO spacer on the specific energy consumption of hybrid RO desalination system* », J. Membr. Sci., vol. 668, p. 121247, February.

[34] C. P. Koutsou, E. M. Kritikos, A. J. Karabelas, et M. Kostoglou, 2020, « *Analysis of temperature effects on the specific energy consumption in reverse osmosis desalination processes* », Desalination, vol. 476, p. 114213, February.

[35] Q. J. Wei, R. K. McGovern, et J. H. L. V, 2017, « *Saving energy with an optimized two-stage reverse osmosis system* », Environ. Sci. Water Res. Technol., vol. 3, n° 4, p. 659-670, June.

[36] E. Hosseinipour, K. Park, L. Burlace, T. Naughton, et P. A. Davies, 2022, « *A free-piston batch reverse osmosis (RO) system for brackish water desalination: Experimental study and model validation* », Desalination, vol. 527, p. 115524, April.

[37] J. Kim, K. Park, D. R. Yang, et S. Hong, « *A comprehensive review of energy consumption of seawater reverse osmosis desalination plants* », Appl. Energy, vol. 254, p. 113652, nov. 2019.

[38] S. Guarino, P. Catrini, A. Buscemi, V. L. Brano, et A. Piacentino, 2023, « *3E assessment of a solar-driven reverse osmosis plant for seawater desalination in a small island of the Mediterranean Sea* », Energy Rep., vol. 10, p. 2260-2276, November.

[39] N. M. Mazlan, D. Peshev, et A. G. Livingston, 2016, « *Energy consumption for desalination — A comparison of forward osmosis with reverse osmosis, and the potential for perfect membranes* », Desalination, vol. 377, p. 138-151, January.

[40] A. Cala, A. Maturana-Córdoba, et J. Soto-Verjel, 2023, « *Exploring the pretreatments' influence on pressure reverse osmosis: PRISMA review* », Renew. Sustain. Energy Rev., vol. 188, p. 113866, December.

[41] A. Bohos, A. Gaydardzhiev, M. Streblau, 2013, « *Study of corrosion resistance of contact rivets of electrical apparatus with nanostructured coatings of the Ti/TiN type* », Journal of Marine Technology and

Environment, vol.2, p.7-12, October, Nautica Publish House, Constanta, Romania.

[42] Ghiocel, A., Panaitescu V., Panaitescu M., Tuleanu, C., 2016, « *Current state of sludge production, management, treatment and disposal in Romania* », Journal of Marine [Technology and Environment, vol.2, p.23-26, October, Nautica Publish House, Constanta, Romania.